High Energy Physics and Nuclear Physics

Volume 19, Number 2

Suppression of Dilepton Production in Expanding Hot Baryon-Rich Quark-Gluon Matter

He Zejun, Zhang Jiaju, and Qiu Xijun

(Institute of Nuclear Research, the Chinese Academy of Sciences, Shanghai, China)

From the full stopping scenario, we have studied the dilepton spectrum on the basis of the (3+1) dimensional RHE, and come to the conclusion that with increasing initial baryon density the dilepton production in invariant masses between 2 m_π to 1 GeV is shown to be suppressed, and an abnormal peak of the dilepton spectrum appears near the invariant mass 0.75 GeV if the baryon-rich quark-gluon matter is indeed created in ultrarelativistic nuclear collisions. These predictions will be tested in future experiments at CERN and Brookhaven.

Key words: baryon-rich quark matter, dilepton spectrum, gluon matter.

1. INTRODUCTION

The ultimate aim of nucleus-nucleus collisions at ultrarelativistic energies is to create a deconfined quark-gluon matter (QGM). The Relativistic-Heavy-Ion Collider (RHIC) being built at Brookhaven offers the possibility to create QGM in the laboratory [1]. Many experimental observables have been suggested as signatures for QGM production. Among them, the dilepton is studied mostly because it does not suffer strong final-state interactions and is expected to retain the information of QGM.

Received on November 8, 1993.

The dilepton spectrum given by previous authors does not depend on the particle distribution in the space [2,3]. Recently, for the system of zero baryon number, authors of [4,5] studied the influence of the nonhomogeneity of the quark distribution in the space-time on dilepton production by adopting the phase-space distribution function under the Boltzmann approximation, which depends on the particle density, and including the equation of the particle number conservation in the relativistic hydrodynamic equations (RHE).

However, experimental and theoretical studies indicate [6] that up to CERN SPS energies the stopping of a sizable amount of baryon occurs, that is, the Bjorken scenario seems not to be realistic for heavy ion collisions at these energies [7]. In fact, at RHIC bombarding energies $\sqrt{s} \leq 200\,A$ GeV recent calculations using microscopic models [8,9] seem to show that the colliding heavy ions may not be fully transparent. Consequently, the baryon density in the QGM does not vanish. Obviously, in this case the dilepton production rate should be, in local thermodynamic equilibrium, a function of both temperature and baryon densities (i.e., densities of the quark and antiquark). The authors of [10] have studied dilepton production based on the hydrodynamic description of heavy ion collisions. Since they take the spatial average of the hydrodynamic equations, the differential hydrodynamic equations with respect to space-time are simplified into ordinary differential equations with respect to the time. Thus, the calculated temperature, particle density, and corresponding reaction rate and the spectrum are functions of the time only. Recently, authors of [6] studied the dilepton production for finite baryon chemical potential (or corresponding baryon density), and found that the ratio of signal to background decreases with increasing chemical potential. The dilepton production of an expanding hot baryon-rich QGM requires further study.

In this work, we study the dilepton spectrum of an expanding hot baryon-rich QGM based on the $(3+1)$ dimensional RHE. To include the nonhomogeneity of the baryon (i.e., quark and antiquark) distribution in space-time, we first adopt the spectrum expression depending on the quark and antiquark distributions in space-time as given in [4,5], then generalize the RHE to include the equation of the baryon number conservation so that it gives both the temperature and the baryon distributions. Therefore, the quark and antiquark distributions are obtained from considering the relation between the quark chemical potential μ_q and the baryon density for the given temperature [11], and from the fact that the chemical potential of the antiquark is $-\mu_q$ in local thermodynamic equilibrium. Hence, we may study the relation between baryon density and dilepton production. We propose here a scenario for the phase transition that somewhat differs from Kapusta's [3]. The law of energy conservation ensures that the energy densities of the two phases are the same at the critical point [3,4,12]. From such a relation, the initial temperature of the hadron phase is determined. According to the treatment of [11], primary gluons and quarks are allowed to fragment into more quark-antiquark pairs before recombining into mesons to ensure the increase of entropy during the phase transition. Here, we also assume that the hadron phase mainly consists of π, thus the initial particle density of the hadron phase is given by the conversion from quarks to π. Moreover, in this work the temperature and particle density are functions of space-time, accordingly, different local regions in the fireball enter the hadron phase across different points of the phase boundary at different times.

In this work, effects of nonhomogeneities of the quark, antiquark, and temperature distributions in space-time, the released latent heat and the fragmentation of the primary gluons and quarks during the phase transition, and the local phase transition based on the phase boundary have been considered.

2. BASIC EQUATIONS

2.1. Dilepton Spectrum Depending on the Baryon Density

To study the effect of the quark and antiquark distributions on the spectrum, we have adopted the particle density-dependent phase-space distribution function under the Boltzmann approximation [13], and obtained the spectrum of the system

$$\frac{dN}{dM} = \iint \left(\frac{dN}{dM d^4X}\right)_B n_1(r,t) n_2(r,t) dr dt \tag{2.1}$$

and the corresponding total yield

$$N(n_0, T_0) = \int \left(\frac{dN}{dM}\right) dM, \tag{2.2}$$

where n_1 and n_2 are densities of the quark and antiquark, respectively. The dilepton production spectrum $(dN/dMd^4X)_B$ is given from Boltzmann distribution function $f(p_i) = c_i \exp(E_i/T)$. Here, Eqs. (2.1) and (2.2) are different from those obtained in [4,5], where $n_1 = n_2$, namely, the baryon number of the system is zero. However, in this work $n_1 > n_2$ (i.e., it is a baryon-rich system). In the following section n_1 and n_2 are given.

2.2. Dynamic Expansion of the QGM

As pointed out in [14], once local thermodynamic equilibrium of the system is established, the evolution of the fireball is governed by the energy-momentum conservation law

$$\partial_\mu (T^{\mu\nu}) = 0, \tag{2.3}$$

where $T^{\mu\nu}$ is the well-known energy-momentum tensor. In general, ε and p depend, in local thermodynamic equilibrium, on the local temperature and baryon density, and the following conservation law for baryons must be included [14]:

$$\partial_\mu (n u^\mu) = 0, \tag{2.4}$$

where $n = \gamma n_r$ is the baryon density, γ the Lorentz contract factor, and n_r the baryon density in the rest-frame. Considering that at the early stage of the evolution of the fireball the mean free paths are small compared with the system size, the viscosities can be neglected, and the entropy of the system should be conserved [14]:

$$\partial_\mu (S u^\mu) = 0, \tag{2.5}$$

By virtue of the thermodynamic relation

$$ds = T dS + \mu_b dn, \tag{2.6}$$

$$dp = S dT + n d\mu_b. \tag{2.7}$$

from (2.3)-(2.5), we obtain the RHE

$$\partial_t S + \frac{1}{r^2}\partial_r (r^2 S \tanh\eta) = 0, \tag{2.8}$$

$$\partial_t n + \frac{1}{r^2}\partial_r (r^2 n \tanh\eta) = 0, \tag{2.9}$$

$$\begin{aligned} ST[\tanh\eta \partial_t \ln T + \partial_r \ln T + \tanh\eta \partial_r \eta + \partial_t \eta] \\ + n\mu_b[\tanh\eta \partial_t \ln \mu_b + \partial_r \ln \mu_b + \tanh\eta + \partial_t \eta] = 0, \end{aligned} \tag{2.10}$$

where η stands for the radial velocity, and μ_b stands for the baryon chemical potential. With the help of a phenomenological MIT-bag model [15], one obtains the relation between the baryon density and the quark chemical potential

$$n = \frac{1}{3}\frac{\partial p_{qg}(\mu_q, T)}{\partial \mu_q} = \frac{2}{3}\mu_q(T^2 + \mu_q^2/\pi^2) \tag{2.11}$$

and the relation between the entropy and the quark chemical potential

$$S = \frac{\partial p_{qg}}{\partial T} = \frac{74}{45}\pi^2 T^3 + 2\mu_q^2 T. \tag{2.12}$$

Using Eqs. (2.11) and (2.12), Eqs. (2.8)-(2.10) become a set of coupled RHE with respect to the temperature, baryon density and radial velocity η. When solving this set of coupled equations, we have given initial values for these three quantities as done in [4,5], but using the baryon distribution instead of the quark distribution. With the help of distributions of the temperature and the baryon density n, we have obtained the quark chemical potential μ_q and antiquark chemical potential μ_q using Eq. (2.11), and then the corresponding phase-space distribution functions $f_q(k)$ and $\bar{f}_q(k)$. Thus, densities of the quark and antiquark of the baryon-rich system are given, respectively, by

$$n_1(r,t) = \int d^3k f_q(k), \tag{2.13}$$

and

$$n_2(r,t) = \int d^3k \bar{f}_q(k). \tag{2.14}$$

Finally, we have calculated the dilepton spectrum and the total yield using Eqs. (2.1) and (2.2).

2.3. Effects in the Phase Transition

In general, the phase boundary is determined by the condition that the temperature, pressure, and baryon chemical potential of the hadron phase and the quark phase are equal. Neglecting the contribution of the strange particle [16], the quark chemical potential is determined by the relation $p_{qg} = p_h$, where p_{qg} is the equation of state of QGM, as given in [11], and p_h is the pressure of the hot pion gas. The phase boundary in the phase diagram n-T is also obtained.

The authors of [4,5] assume that the nucleation rate is so large that once the local value (n,T) of the quark fireball reaches the phase boundary values the QGM makes a sudden transition to the hadron matter at the temperature T_h. The law of energy conservation requires that the energy densities of the two phases are the same at the critical point. From such a relation T_h is determined and regarded as the initial value of the hadron phase.

To conserve the entropy during the phase transition, we adopt the concept given in [11], which assumes that primary gluons and quarks are allowed to fragment into more quark-antiquark pairs before recombining into hadron matter to compensate for the decrease of the entropy. In this calculation, we have adopted fragmentation parameters as used in [17].

The authors of [18] have assumed that a quark pair converts into a pion with 75% probability and into a η or η' meson with 25% probability. Further considering the $\eta \to 3\pi$, $\eta' \to 3\pi$, and $\eta \to \pi^+\pi^-\pi^0$ processes [19], we have assumed the effective probability of 80% for a quark pair converting into a pion [4,5].

3. CALCULATED RESULTS AND DISCUSSIONS

The calculated phase boundaries are shown in Fig. 1; curve 1 is obtained for the bag constant $B^{1/4}$

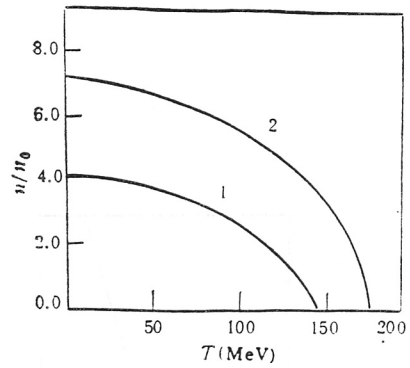

Fig. 1

Phase diagram. Curves 1 and 2 are, respectively, phase boundaries for the bag constants $B^{1/4}$ = 200 MeV and 240 MeV.

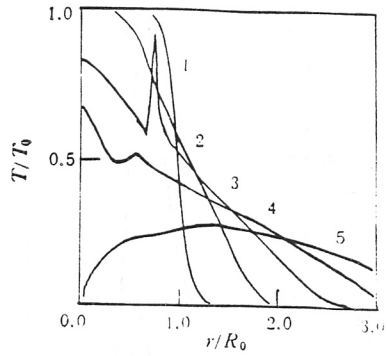

Fig. 2

The evolution of the temperature of the quark-gluon fireball for the critical temperature T_c = 160 MeV. Curves 1-5 are, in turn, temperature distributions at the initial temperature T_0 = 250 MeV for $1/R_0$ = 0.0, 0.6, 1.2, 1.5, 1.8, and 2.4, where t is the time R_0, the initial radius of the fireball.

= 200 MeV, curve 2 for $B^{1/4}$ = 240 MeV.

For convenience, we only show the temperature distribution of the system in Fig. 2 for the case in which the phase transition occurs at the point (T_c,0) of the phase boundary. It is shown that the latent heat significantly enhances the temperature of the system. T_c is the temperature at the crossing between the phase boundary and the temperature axis. The distribution of the baryon density is shown in Fig. 3. We see that the total baryon number obtained by integrating the distribution of the baryon at any time over the volume of the fireball is a constant with respect to the time. It shows that in our calculation the baryon number conservation is satisfied.

In Fig. 4, we have shown the invariant mass spectra from $^{197}Au+^{197}Au$ central collisions for the phase boundary 1 at the initial temperature T_0 = 120 MeV. Curves 1 to 6 denote, in turn, spectra for the initial baryon densities n_0 = 1-6 × n_N, where n_N is the normal nuclear density. If the system has initial values (n_0, T_0) in the quark phase, the evolution of the system must undergo the phase transition.

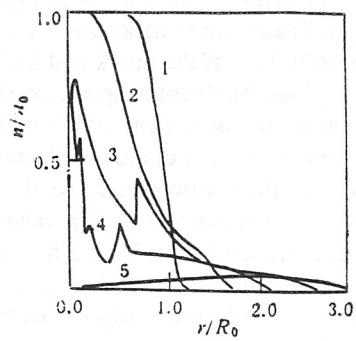

Fig. 3

The calculated distribution of the baryon under the same parameters as given in Fig. 2.

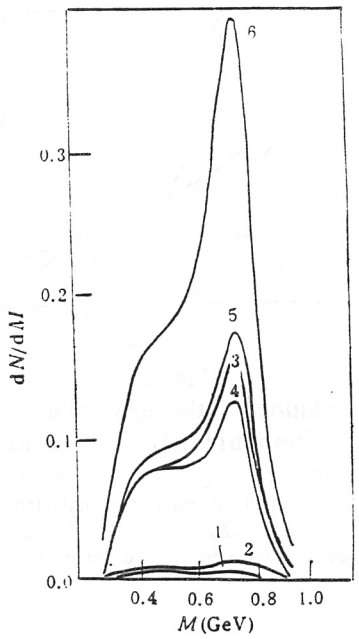

Fig. 4

The dilepton invariant mass spectrum calculated according to the phase boundary 1 given in Fig. 1. Curves 1-6 are, in turn, dilepton invariant mass spectra for the initial temperature T_0 = 120 MeV and initial baryon densities n_0 = 1-6 × n_N and n_N is the normal nuclear density 0.17 fm^{-3}.

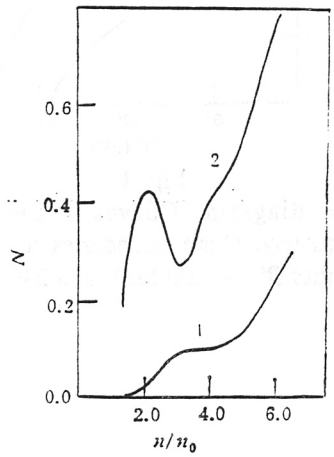

Fig. 5

The dilepton total yield as a function of the initial baryon density. Curve 1 is obtained from the phase boundary 1 in Fig. 1 at the initial temperature T_0 = 120 MeV, curve 2 from the phase boundary 2 in Fig. 1 at T_0 = 178 MeV. n/n_0 denotes the ratio of the initial baryon density to the normal nuclear density.

For spherically symmetric expansion, the phase transition occurs only in a local spherical shell outside the central quark region, where the temperature and baryon density are enhanced largely due to the release of the latent heat and fragmentation of the particles, thus the initial value and contribution of the hadron phase increase so greatly that an abnormal peak near invariant mass 0.75 MeV is produced. On the other hand, from the particle diffusion and thermal conduction, the heat in the shell necessarily enters the central quark region to increase the temperature of the quark phase as seen in Fig. 2, whereas particles in the shell tend to resist the outward motion of quarks in the central region to keep the occupation number of quarks high. These effects delay the evolution process, increase the lifetime of the system, and lead to larger contributions of the quark and hadron phase. Therefore, the system with initial values in the quark phase gives the dilepton spectrum shown as curve 3 in Fig. 4, which is much higher than curves 1 and 2 given by the system with initial values in the hadron phase.

From Fig. 4, we see that with further increase of the initial baryon density, the gradient between the density in the central quark region and the one outside the shell, where the phase transition occurs, gets larger. As the initial baryon density increases to a certain value, the outward motion of particles in the central region is accelerated and predominates. Thus, the lifetime of the system shortens, the dilepton production rapidly decreases, and curve 4 is under curve 3. If we continue to increase the initial baryon density, the influences of quark and antiquark occupation numbers on the dilepton production become predominant. Since the primary quark and antiquark numbers increase, quark-antiquark pairs after fragmentation also increase. This makes the dilepton yield go up again monotonically with the initial baryon density. Therefore, we see in Fig. 4 that the change of the

dilepton spectrum versus the initial baryon density is nonmonotonic. The same characteristic spectrum is obtained at the initial temperature T_0 = 178 MeV for phase boundary 2 in Fig. 1.

From the experimental point of view, we should give the total dilepton yield. The results given in Fig. 5 more clearly show that the dilepton production is nonmonotonic versus the initial baryon density.

In conclusion, if the baryon-rich QGM was created in the collision, the dilepton production of the system must have the following characteristics: with the increase of the initial baryon density, once the system enters the quark phase from the hadron phase, the dilepton production increases suddenly, the dilepton spectrum peaks abnormally near the invariant mass 0.75 MeV, and dilepton production undergoes a suppression, making a plateau or valley in the invariant mass region of $2m_\pi$ to 1 GeV. These characteristics will be tested in the experiments at CERN and Brookhaven.

REFERENCES

[1] S. Ozaki, *Nucl. Phys.*, **A525**(1991): p. 125c.
[2] S. A. Chin, *Phys. Lett.*, **B119**(1982): p. 51.
[3] J. Kapusta and A. Mekjian, *Phys. Rev.*, **D33**(1986): p. 1304.
[4] Zejun He, Jiaju Zhang, Panlin Li *et al.*, *Nucl. Phys.*, **A532**(1991): p. 743.
[5] Zejun He, Jiaju Zhang, Panlin Li *et al.*, *J. Phys. G: Nucl. Part.*, **16**(1990): p. L179.
[6] A. Dumitru, D. H. Rischke *et al.*, *Phys. Rev. Lett.*, **70**(1993): p. 2860.
[7] J. D. Bjorken, *Phys. Rev.*, **D27**(1983): p. 140.
[8] G. Gustafson, 1992. Proceedings of the workshop on relativistic heavy ion physics at present and future accelerators, Budapest.
[9] H. J. Möhring and J. Ranft, *Z. Phys.*, **C52**(1991): p. 643.
[10] Ko C. M. and Xia L. H., *Phys. Rev. Lett.*, **62**(1989): p. 1595.
[11] P. Koch, B. Müller, and J. Rafeski, *Phys. Rep.*, **142**(1986): p. 169.
[12] K. Kajantie, M. Kataja *et al.*, *Phys. Rev.*, **D34**(1986): p. 811.
[13] J. E. Mayer and M. G. Mayer, *Statistical Mechanics*, 2nd ed. New York: Wiley, 1977.
[14] G. Baym, B. L. Friman, J. P. Blaizot *et al.*, *Nucl. Phys.*, **A407**(1983): p. 541.
[15] K. Kubodera, J. Delorme, M. Rho, *Phys. Rev. Lett.*, **40**(1978): p. 755.
[16] K. S. Lee, M. J. Rhoades-Brown, and U. Heinz, *Phys. Lett.*, **B174**(1986): p. 123.
[17] Zejun He, Jiaju Zhang *et al.*, *J. Phys., G: Nucl. Part. Phys.*, **19**(1993): p. L7.
[18] H. W. Barz, B. L. Friman *et al.*, *Nucl. Phys.*, **A484**(1988): p. 661.
[19] P. Castoldi and J. M. Frere, *Z. Phys.*, **C40**(1988):p. 283.